# Characterization of a 3-D Photonic Crystal Structure Using Port and S-Parameter Analysis

M. Dong*[1], M. Tomes[1], M. Eichenfield[2], M. Jarrahi[1], T. Carmon[1]

[1]University of Michigan, Ann Arbor, MI, USA
[2]Sandia National Laboratories, Albuquerque, New Mexico, USA
*Corresponding author: 3115 ERB, Ann Arbor, MI 48105, USA, markdong@umich.edu

**Abstract:** We present a 3-D port sweep method in a lossy silicon photonic crystal resonator to demonstrate the capabilities of COMSOL's frequency domain analysis with input and output ports. This method benefits from the advantages of the S-parameter analysis to characterize the input and output coupling into the resonator. By pumping one end of the cavity with a CW plane wave, we are able to extract the total reflection and transmission coefficients through our cavity, the band gap edges of the photonic crystal, and the quality factor of the resonance. We also sweep the lattice constants and reflector periods of the photonic crystal to optimize our coupling into the cavity, achieving critical coupling.

**Keywords:** photonic crystals, optical cavity, coupling, ports, s-parameter

## 1. Introduction

Numerical simulations[1] are common in describing optical experiments in microdevices. Among them, light tunneling[2], optical level crossing[3], and generation of 3rd [4] and 4th [5] harmonics. In the mechanical domain, simulations of vibrational modes in microresonators [6,7] provide details on recently observed mechanical whispering-gallery modes [8,9] that are electrostictivly excited by light as well as on the traditional breath modes [10] that are excited by the centrifugal radiation pressure that the circulating light applies on the device walls. Numerical simulations also describe optomechanical crystals [11] and optomechanics in microfluidic devices [12,13]. In COMSOL, the use of its eigenfrequency solver has been predominant in these characterizations, giving us the resonance frequency, field profile, and quality factor of the eigenmode. However, in order to model our real experiments more accurately, knowing the input and output coupling to these resonators is critical to ensuring we get adequate power that can decouple out of the cavity and reach the detector. This is particularly important in lossy cavities and systems where asymmetric input and output coupling has advantages.

In this study, we use an alternative approach involving input and output ports in COMSOL to characterize our optical cavity that complements the eigenfrequency solver. For our demonstration, we adapt a silicon photonic crystal cavity design [14] to terahertz frequencies (100 GHz). At such frequencies, silicon material losses are significant and port based simulations can offer additional insight to coupling.

## 2. Background

The photonic crystal band gap originates from solving the eigenvalue Helmholtz equation for the electric field

$$\nabla \times \nabla \times \boldsymbol{E}(\boldsymbol{r},t) - \frac{\omega^2}{c^2} n^2(\boldsymbol{r}) \boldsymbol{E}(\boldsymbol{r},t) = 0$$

with a spatially periodic refractive index. The periodic refractive index opens gaps in the band structure where certain frequencies cannot propagate. By modifying the periodicity of the structure between different regions in our device, the range of allowed frequencies is tuned. This allows certain regions to act as mirrors of a cavity. The reflectivity of such mirrors can then be tuned by changing the size of the non-propagating regions.

To make our cavity, we follow the geometry in Figure 1, a triangular lattice with $a$ representing the lattice constant of the central cavity, $a_r$ representing the lattice constant of the reflector region which is related to the cavity constant by the relation $a_r = a_{frac} * a$, and $a_m$ representing the lattice constant of a "matching" region and is equal to the average of $a$ and $a_r$.

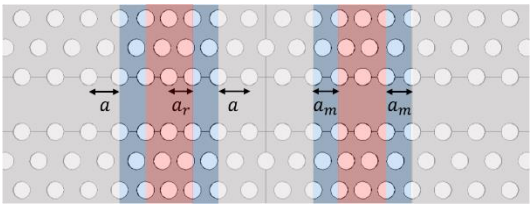


**Figure 1.** Exaggerated geometry of our system, a symmetric silicon photonic crystal cavity. The grey, red, and blue colored regions represent the cavity, mirror, and matching regions. Likewise, $a$, $a_r$, and $a_m$ are lattice constants of the cavity, mirror, and matching regions respectively of the photonic crystal. There are three periods of reflector lattice constant on each side.

The smaller lattice constant of the reflector regions shifts the band gap in those regions relative to the cavity eigenfrequency (with a different lattice constant). The band gap is shifted such that the cavity center frequency cannot propagate through the reflector regions. This means they act as high reflectivity mirrors.

The two mirror regions and the cavity can then be modeled as a lossy fabry-perot interferometer, whose overall intensity transmission and reflection are described by the well-known Airy formulas

$$\frac{I_t}{I_0} = \frac{T_{in}T_{out}(1+e^{-\alpha 2d})}{2\left(1-\sqrt{R}\right)^2} \times \left[1+\frac{4\sqrt{R}}{\left(1-\sqrt{R}\right)^2}\sin^2\left(2\pi d\nu\frac{n(\nu)}{c}\right)\right]^{-1}$$

$$\frac{I_r}{I_0} = \frac{R_{in}+\frac{R}{R_{in}}-2\sqrt{R}\cos\left(\frac{4\pi d\nu n(\nu)}{c}\right)}{1+R-2\sqrt{R}\cos\left(\frac{4\pi d\nu n(\nu)}{c}\right)}$$

where $d$ is the cavity length, $\nu$ is the frequency of light, $n(\nu)$ is the refractive index, $c$ is the speed of light in vacuum, $R_{in}$, $R_{out}, T_{in}, T_{out}$ are the reflection and transmission coefficients, and $R = R_{in}R_{out}e^{-\alpha 2d}$ is the round trip cavity loss with $\alpha$ being the absorption coefficient. It is important to note that from the Airy formulas of a fabry-perot cavity, we find that at certain mirror reflectivities the power reflection reduces to zero, a characteristic of perfect impedance matching or critical coupling. The reflected intensity becomes zero on resonance in the reflected intensity equation when $R_{in} = R_{out}e^{-\alpha 2d}$, meaning the input mirror should be slightly less reflective than the output to achieve critical coupling.

Beyond these mirror regions lies a waveguide region in which the lattice constant returns to the value of the cavity, allowing us to send light through the waveguide and couple into the cavity.

## 3. Numerical Modeling

We use COMSOL Multiphysics *Radio-Frequency Module* (RF), version 4.3a to first numerically solve the electric eigenvalue equation in order to find the eigenfrequency of our cavity, and then using ports to excite a plane wave into the cavity to calculate the S-parameters and characterize the coupling. The important simulation parameters are given in Table 1. Note that $N_{rl}$ and $N_{rr}$ are the number of reflector periods on the left (input) and right (output) side respectively.

**Table 1:** Simulation Parameters

| Parameter | Value | Units |
|---|---|---|
| $a$ | 0.784 | mm |
| $a_{frac}$ | 0.9763 | 1 |
| $a_m$ | 0.7747 | mm |
| $N_{rl}$ | 3 | 1 |
| $N_{rr}$ | 3 | 1 |
| $n_{si}$ | 3.42 | 1 |
| $\alpha$ | 0.01 | $\text{cm}^{-1}$ |

The refractive index model is used for all simulations and the real index and per length loss of silicon are both listed.

The governing equations solved in the eigenfrequency solver and the port simulation are the frequency domain versions of Maxwell's equations for a non-magnetic material in a time harmonic field

$$\nabla\times\nabla\times\boldsymbol{E}(\boldsymbol{r},\omega) - \frac{\omega^2}{c^2}n^2(\boldsymbol{r})\boldsymbol{E}(\boldsymbol{r},\omega) = 0$$

$$\nabla\times\left(\frac{1}{n^2(\boldsymbol{r})}\nabla\times\boldsymbol{H}(\boldsymbol{r},\omega)\right) - \frac{\omega^2}{c^2}\boldsymbol{H}(\boldsymbol{r},\omega) = 0$$

The simulation is set up to calculate only a quarter of the full geometry. The boundary conditions are such that we solve for only the vertically polarized

light traveling through the waveguide and into the cavity.

## 4. Results

The results of the eigenfrequency and port simulations are given in Figure 2 for the parameter values given in Table 1. The port simulation shows the photonic crystal band gap with a resonance near the edge. The resonance frequency in the power reflection and transmission plot is verified to be the cavity resonance found in the eigenfrequency solver.

Figure 3 shows the field and intensity profiles from the port simulation at resonance frequency. The fields inside the cavity are similar to those found using the eigenfrequency simulation in Figure 2 but now show fields coupling in and out on the left and right sides respectively. The steady-state intensity shows some light reflecting back out the input side as the input coupling is not optimized.

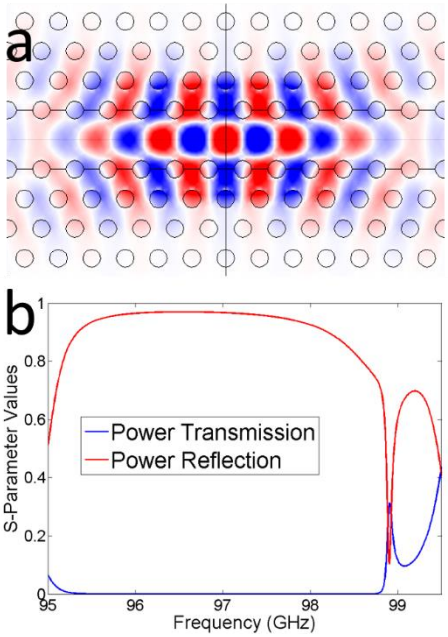


**Figure 2.** a) Field profile of the cavity mode from eigenfrequency analysis b) Power reflection and transmission ($|S_{11}|^2$ and $|S_{21}|^2$) at different frequencies obtained from the port sweep simulation

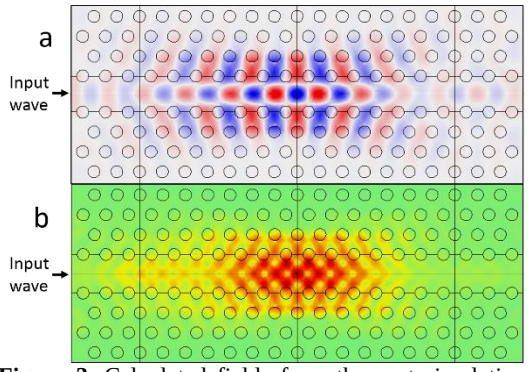


**Figure 3.** Calculated fields from the port simulation using parameters from Table 1. Wave excitation is from the left side without coupling optimization. a) Vertically polarized component of electric field b) Steady state intensity inside the photonic crystal.

## 5. Optimization and Discussion

While the initial study verifies the validity of our port simulation, the photonic crystal cavity can be further characterized in order to achieve an optimized design. We proceed to sweep a few of the parameters listed in Table 1 and plot the changes to the overall power transmission and reflection.

The transmission coefficient through the photonic crystal as $a_{frac}$is being swept is shown in Figure 4. Notice that as $a_{frac}$ becomes closer to 1, meaning as the reflector region's lattice

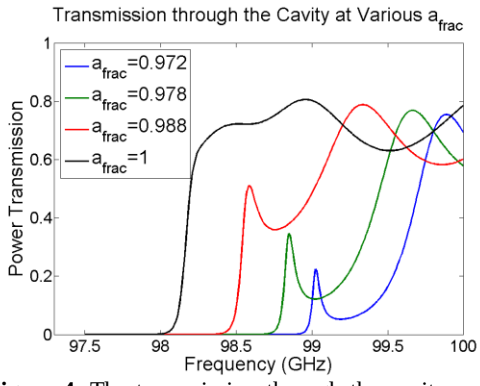


**Figure 4.** The transmission through the cavity as the parameter $a_{frac}$ is swept from its initial value to 1. This also changes the reflector region's lattice constant as defined $a_r = a_{frac} * a$ which then changes the matching region's lattice constant as defined $a_m = \frac{a_r + a}{2}$

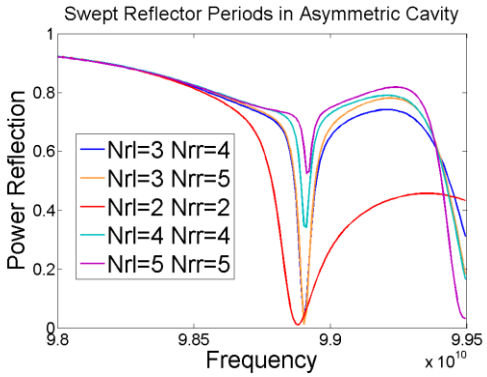


**Figure 5.** The power reflection coefficient as the number of reflector periods on the left side ($N_{rl}$) and the right side ($N_{rr}$) are swept, with $a_{frac} = 0.9763$.

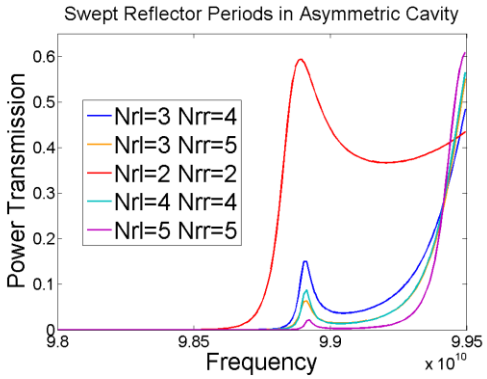


**Figure 6.** The power transmission coefficient as the number of reflector periods on the left side ($N_{rl}$) and the right side ($N_{rr}$) are swept. $a_{frac} = 0.9763$ in these simulations

constant is approaching that of the cavity region, the mode is becoming less and less confined as the reflectivity of the mirrors is effectively decreasing, eventually disappearing altogether when $a_{frac} = 1$. The quality factor also decreases as the mirror reflectivity is decreasing. Total transmission however is increasing when the mode becomes less confined.

While shifting the band gap can change the mirror reflectivity, we can also change the reflectivity by changing the number of reflector periods on both sides of the cavity.

Figure 5 and Figure 6 show some results of the swept reflector periods. We also see the power reflectivity dropping to very nearly zero indicating critical coupling, particularly for the parameter values $N_{rl} = 3, N_{rr} = 4$ and $N_{rl} = 3, N_{rr} = 5$. This agrees with the critical coupling requirement as mentioned earlier that the input

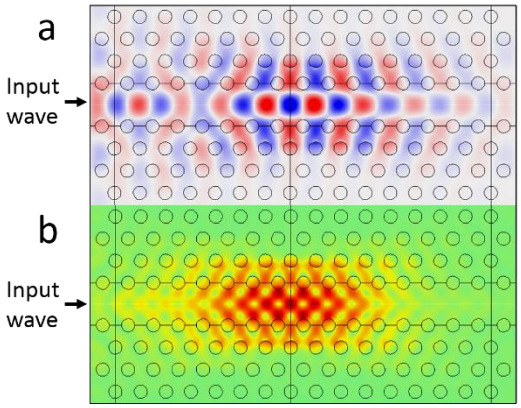


**Figure 7.** Calculated fields from the port simulation with parameters $N_{rl} = 2, N_{rr} = 2$ and $a_{frac} = 0.9763$ Wave excitation is from the left side. a) Vertically polarized component of electric field b) Steady state intensity inside the photonic crystal.

mirror be slightly less reflective than the output mirror. The quality factors for these two pairs has also not degraded due to low mirror reflectivity. However, despite the quality factor being nearly the same, the power transmission plot shows the second pair ($N_{rl} = 3, N_{rr} = 5$) having a much worse overall transmission through the cavity. This is due to the larger mirror reflectivity from the higher number of reflector periods on the output end.

In addition, for low values of reflector periods, the resonances display a low quality factor due to low reflectivity, similar to the results from $a_{frac}$ sweep. The parameter value of $N_{rl} = 2, N_{rr} = 2$ illustrates the significantly wider resonance peak, suggesting a very weak cavity with a large portion of the input light tunneling through the mirrors. Despite being a symmetric cavity, this pair also has the low reflectivity that is characteristic of critical coupling. This is due the $N_{rl} = 2, N_{rr} = 2$ pair being much less reflective overall so the material loss inside the cavity becomes less significant in disrupting the symmetry.

The field profile of the almost critically coupled cavity is also plotted again for comparison in Figure 7. In the steady state intensity plot, the magnitude of the reflected fields back towards the input port is less than those shown in Figure 3, consistent with the calculated power reflection at this frequency.

## 6. Conclusion

We have characterized many important aspects of a photonic crystal cavity using the port and S-parameter capabilities of COMSOL Multiphysics. Although we only show the results of sweeping a few parameters, many other parameters in this photonic crystal cavity can be changed to see how they affect the overall transmission through the cavity. We hope that this method will be useful in the characterizations of other resonator systems, particularly if finding the coupling efficiency is of interest.

## 7. Acknowledgements

This work is supported by the National Science Foundation. We would also like to acknowledge the University of Michigan for their software support and services.

## 8. References

1. M. Oxborrow, Traceable 2-D finite-element simulation of the whispering-gallery modes of axisymmetric electromagnetic resonators, *IEEE Transactions on Microwave Theory and Techniques*, **55(6)**, 1209-1218 (2007)
2. M. Tomes et al., Direct imaging of tunneling from a potential well, *Optics Express*, **17**, 19160 (2009)
3. T. Carmon et al., Static envelope patterns in composite resonances generated by level crossing in optical toroidal microcavities, *Phys. Rev. Let.*, **100**, 103905 (2008)
4. T. Carmon, K. J. Vahala, Visible continuous emission from a silica microphotonic device by third-harmonic generation, *Nature Physics*, **3(6)**, 430-435 (2007)
5. J. Moore et al., Continuous-wave ultraviolet emission through fourth-harmonic generation in a whispering-gallery resonator, *Optics Express*, **19(24)**, 24139-24146 (2011)
6. J. Zehnpfennig et al., Surface optomechanics: Calculating optically excited acoustical whispering gallery modes in microspheres, *Optics Express*, **19**, 14240-8 (2011)
7. G. Bahl et al., Acoustical whispering-gallery modes in optomechanical shells, *New Jour. of Phys.*, **14**, 115026 (2012)
8. G. Bahl et al., Stimulated optomechanical excitation of surface acoustic waves in a microdevice, *Nat. Comm.*, **2**, 403 (2011)
9. M. Tomes, T. Carmon, Photonic micro-electromechanical systems vibrating at X-band (11GHz) rates, *Phys. Rev. Let.*, **102(11)**, 113601 (2009)
10. T. Carmon et al., Temporal behavior of radiation-pressure-induced vibrations of an optical microcavity phonon mode, *Phys. Rev. Let.*, **94**, 223902 (2005)
11. M. Eichenfield et al., Optomechanical Crystals, *Nature*, **462(7269)**, 78-82 (2009)
12. G. Bahl et al., Brillouin cavity optomechanics with microfluidic devices, *Nat. Comm.*, **4**, 1994 (2013)
13. K. H. Kim et al., Cavity optomechanics on a microfluidic resonator with water and viscous liquids, *arXiv*, 1205.5477 (2012)
14. B. Song et al., Ultra-high-Q photonic double-heterostructure nanocavity, *Nature Materials*, **4(3)**, 207-210 (2005)